Effect of Decay on Ultrasonic Velocity and Attenuation Measurements in Wood

by Megan McGovern*, Adam Senalik*, George Chen†, Frank C. Beall‡ and Henrique Reis§

ABSTRACT

The percentage mass loss of loblolly pine ***(Pinus taeda)*** wood cube specimens exposed to Gloeophyllum fungus ***(Gloeophyllum trabeum)*** for increasing periods of time ranging from 1 to 12 weeks was recorded after being subjected to controlled decay following ASTM International standard ***ASTM D 1423-99.*** The specimens' corresponding volume loss due to decay and corresponding densities were calculated using X-ray computed tomography. Blocks decayed for 12 weeks experienced, on the average, the greatest loss of mass (≈40%), volume (≈30%) and density (≈37%). For each of the three principal material directions of these specimens with controlled decay, ultrasonic longitudinal and shear velocity values, along with the corresponding attenuation values, were measured using longitudinal and shear ultrasonic transducers with a center frequency of 100 kHz. Because of the relatively small size of the wooden specimens, a steel delay line was used, along with waveform averaging and the phase-comparison technique, to measure velocities. It was observed that the velocities increased with increasing frequency and decreased with increasing amount of decay, while the corresponding attenuation values increased with increasing frequency and amount of decay. Towards estimation of velocity and attenuation values, polynomial expressions fitted to the experimentally obtained data are presented for the frequency band of 4.5 to 200 kHz and up to a mass loss of 40%.

KEYWORDS: loblolly pine, wood, wood decay, rot, X-ray computed tomography, wood density.

Introduction

The process of wood decay in wooden structures jeopardizes their structural fitness-for-service, creating risks to human life and property (Goodell, 2003; Goodell and Xu, 2000; Green and Highley, 1996). There have been several attempts to inhibit the decay process from occurring altogether. However, the best preservative techniques available today have not been able to truly preserve wood or wood composites against the natural process of decay (Curling et al., 2002; Eaton and Hale, 1993; Highley, 1999; Koenigs, 1974; Tanaka et al., 1994). Wood decay causes the expenditure of significant financial resources annually in repair, rehabilitation and reconstruction efforts. For example, in the United States there are more than 42 million wooden utility poles for power distribution purposes. These poles are commonly deteriorated by fungi, which effectively decay (or rot) the wood. One major U.S. power supplier owns approximately 2.4 million utility poles (Beall et al., 1994). Assuming an approximate replacement cost of $2000 per pole, a 1% reduction of removals would save approximately $240 000 annually. The natural process of wood decay is also occurring in real estate structures, where millions of dollars in wooden real state transactions occur daily without being inspected for decay, and in other wooden infrastructures such as telephone poles, bridges, piles and so on. This decay process decreases the dynamic strength

* Department of Industrial and Enterprising Systems Engineering, University of Illinois, 104 S. Mathews Ave., Urbana, Illinois 61801; (217) 333-1228; fax (217) 244-5705.

† U.S. Department of Agriculture, Forest Products Laboratory, 1 Gifford Pinchot Dr., Madison, Wisconsin 53726.

‡ University of California at Berkeley, Forest Products Laboratory, 1301 S. 46th St., Richmond, California 94804.

§ Department of Industrial and Enterprising Systems Engineering, University of Illinois, 104 S. Mathews Ave., Urbana, Illinois 61801; (217) 333-1228; fax (217) 244-5705; e-mail h-reis@illinois.edu.

of the wood considerably, which can also lead to unexpected failures. For a comprehensive literature review of wood decay, see outside references (Beall et al., 1994; McGovern, 2011; Senalik et al., 2010; Titta et al., 1998).

For wood decay to occur, it only requires the presence of moisture with the appropriate temperature (Cowling, 1961; Highley, 1977; Goodell, 2003; Goodell and Xu, 2000; Green and Highley, 1996). During decay, there is a significant amount of mass loss (the longer the exposure to decay, the larger the mass loss), as well as stiffness and strength loss (Curling et al., 2002). As a result, monitoring wood decay is necessary for ensuring structural serviceability and safety requirements. To date, no practical nondestructive testing and evaluation technique has proven able to detect and monitor in situ the entire decay process of wooden structural components. Typically, these techniques detect decay only when it is already visible on the surface of wooden components, which by then are already in an advanced state of decay and do not need advanced detection techniques.

ASTM D 1413 was developed to determine the minimum amount of preservative that is effective in preventing (that is, delaying) decay of selected wood species by selected fungi under optimum laboratory conditions (ASTM, 2003). In this paper, 25.4 mm loblolly pine ***(Pinus taeda)*** wooden cubes (without any preservatives) were exposed to *Gloeophyllum trabeum* fungus from periods of 1 to 12 weeks. The amount of decay (that is, mass loss) was then evaluated using *ASTM D 1413* (ASTM, 2003).

While ultrasonics and acousto-ultrasonics have shown the potential to detect and assess wood decay, there is no comprehensive published data regarding the change in velocity and attenuation values as a function of mass loss caused by wood decay (Beall et al., 1994; Senalik et al., 2010; Titta et al., 1998). This paper addresses this need for loblolly pine wood *(P.taeda)*.

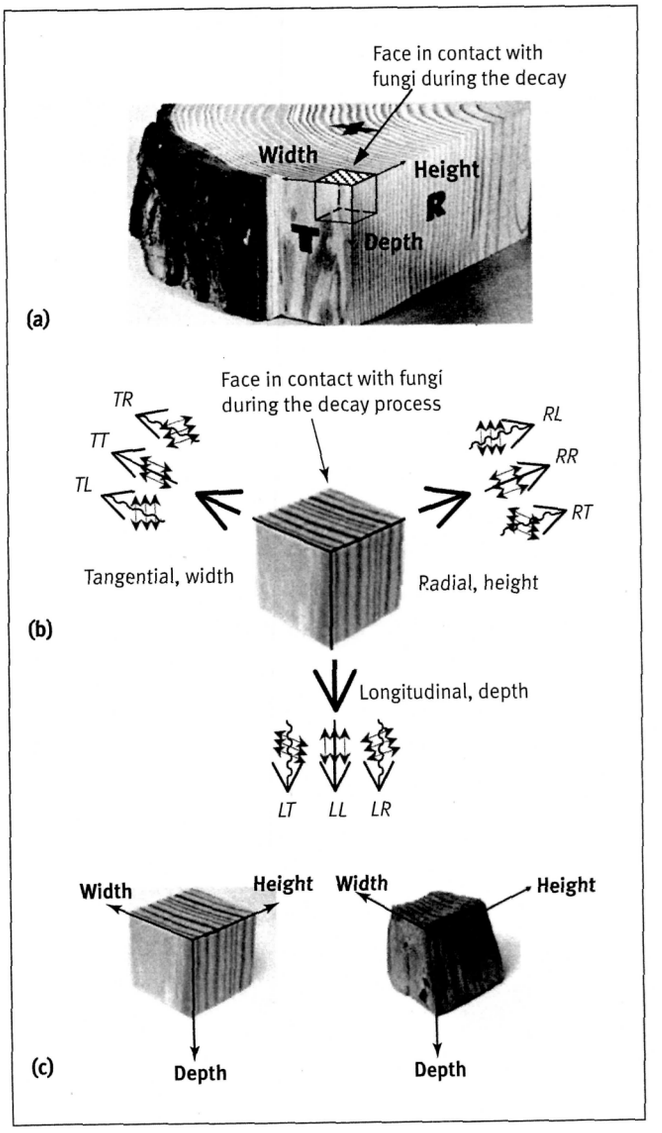

Figure 1. Wood block specimens: (a) assigned reference coordinate system for the wooden cubes and terminology used in this study; (b) the three principal material axes and three different wave polarization for each axis; and (c) block of sound wood (left) versus block of wood exposed to 10 weeks of controlled decay (right).

Test Specimens and Results *using ASTM D 1413*

ASTM D 1413 was used to obtain wooden specimens with decay under controlled conditions. Loblolly pine wood *(P. taeda)* was cut into 70 cube block specimens, 25.4 mm on each side, as in Figure 1a. The wooden cubes were brought to constant moisture equilibrium of 30% relative humidity at 300 K (27 °C) for three weeks, and their weight was measured to the nearest 0.01 g prior to submitting them to the process of decay. A wood-destroying fungus *(G. trabeum)* was grown on a feeder strip. Ten blocks were not exposed to the decay process and were labeled as control blocks. The remaining 60 blocks were divided into 12 groups of five block specimens each and were placed in contact with the feeder strip. The blocks were oriented with the grains perpendicular to the plane of the strip, as illustrated in Figure 1a, which also illustrates the coordinate system assigned to the blocks used in this study. These 12 groups of five blocks each remained in contact with the feeder strip from one week up to 12 weeks.

At the end of each week, one group of five blocks was removed, and each of the five blocks was weighed to the nearest 0.01 g. Figure 1b shows the three principal material axes and the three different wave polarizations associated with each of the axes used during mechanical wave testing. Figure 1c shows two blocks for visual comparison; one block has no decay and the other was exposed to the controlled decay process for 10 weeks.

Figure 2a shows the percent of mass loss for the wooden blocks after being submitted to the process of controlled decay from 1 to 12 weeks. In Figure 2a, the error bars represent two standard deviations. Please note that the post-decayed

mass of some of the block specimens subjected to only one week of controlled decay were higher than the original mass, perhaps caused by the initial moisture absorption. Figure 2a clearly indicates that the specimens continuously lost mass during the decay process. While *ASTM D 1413* provides a technique for evaluating wood species more resistant to the natural process of decay, or to evaluate the effectiveness of different wood treatments against wood decay, the standard only provides the final value of mass loss for each specimen. It does not clarify the transition between the sound and decayed wood within each specimen or how the decay progresses within the specimen. To evaluate the decay process, X-ray computed tomography of the wood block specimens was also carried out.

X-ray Computed Tomography

A computed tomography scanner was used to scan the block specimens with a rotation of 0.8 s, a field of view of 269 mm and a slice thickness of 1.25 mm at 80 kV and 45 mA. Volume calculations were carried out for each block exposed to the controlled decay process using the computed tomography scan data. Figure 2b shows the normalized volume of the specimens computed using the computed tomography scan data, where the length of the error bars represented two standard deviations. The approximations during the volume calculations using computed tomography data introduced the most error. For the pixel dimension at 0.52 mm, and a slice depth of 1.25 mm, the upper bound of the total possible error in the volume calculations using the computed tomography data was 5.8%. To further reduce this error would require a decrease in slice depth and an increase in pixel resolution. The local density for each wooden block was computed using the computed tomography data and the measured mass of the wood block specimens after being exposed to the controlled process of decay. Figure 2c shows the computed specimen volume average density normalized to the original density for each group to illustrate the approximate average density loss. Again, in Figure 2c the lengths of the error bars are equivalent to two standard deviations.

Visual inspection of the wood block specimens subjected to decay under controlled conditions led to the observation that wood decay does not occur in a uniform manner. The process of decay starts at the surface in contact with the fungi and progresses towards the opposite surface. Figure 1c, a visual comparison between a block subjected to 10 weeks of decay and one of the control blocks, clearly shows this phenomenon. Note the difference in color between the two. It can visually be seen on the decayed block that the material associated with the face in contact with the fungi has experienced a significantly larger volume decrease than the material on the opposite face. As a result, the decayed blocks are not perfect cubes, as they became increasingly distorted the longer they were exposed to the fungi. Note that the volume and density loss increased (in general)' with the number of

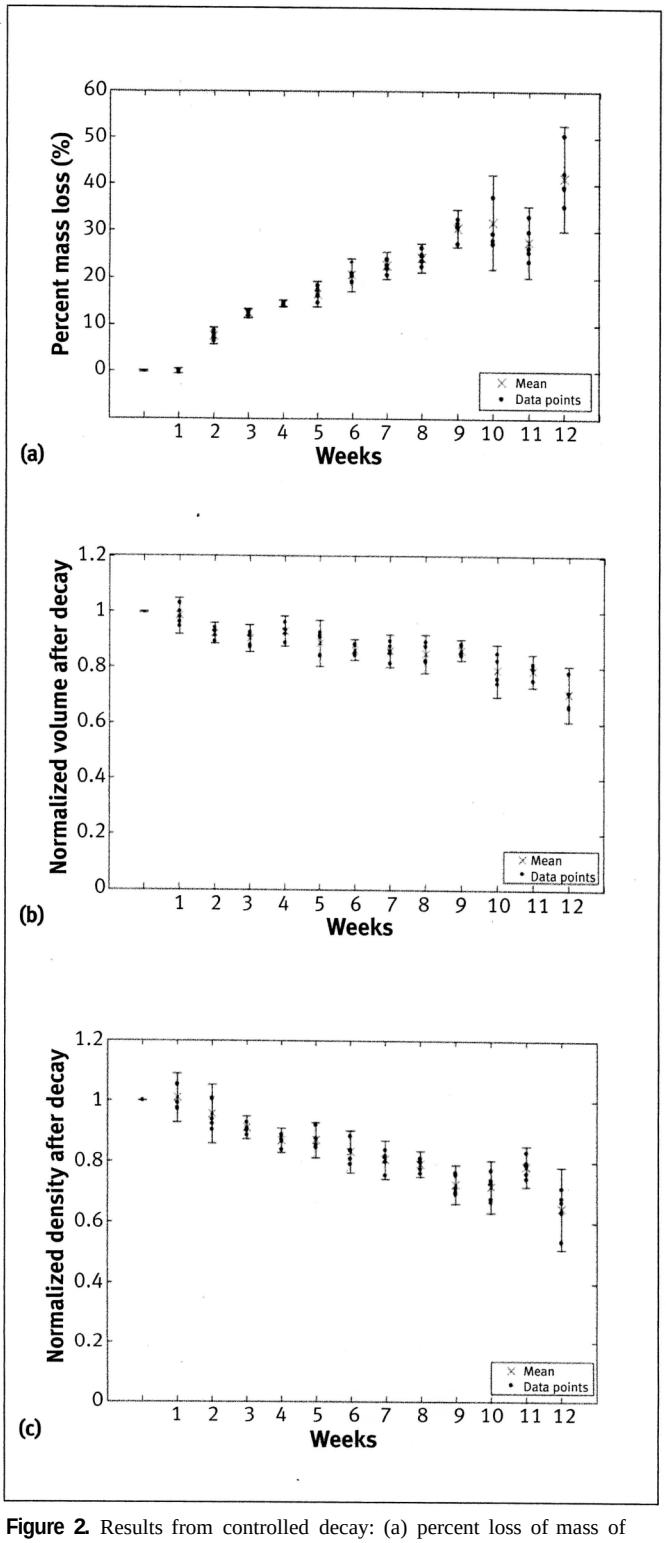

Figure 2. Results from controlled decay: (a) percent loss of mass of blocks after being subjected to controlled decay; (b) volume after decay normalized to the original value of 16.4 mm^3. where the volume of the specimens was calculated using X-ray computed tomography data; and (c) volume average density of each specimen after decay normalized to its original density (assuming an original volume of 16.4 mm^3). Lengths of the error bars are equivalent to two standard deviations.

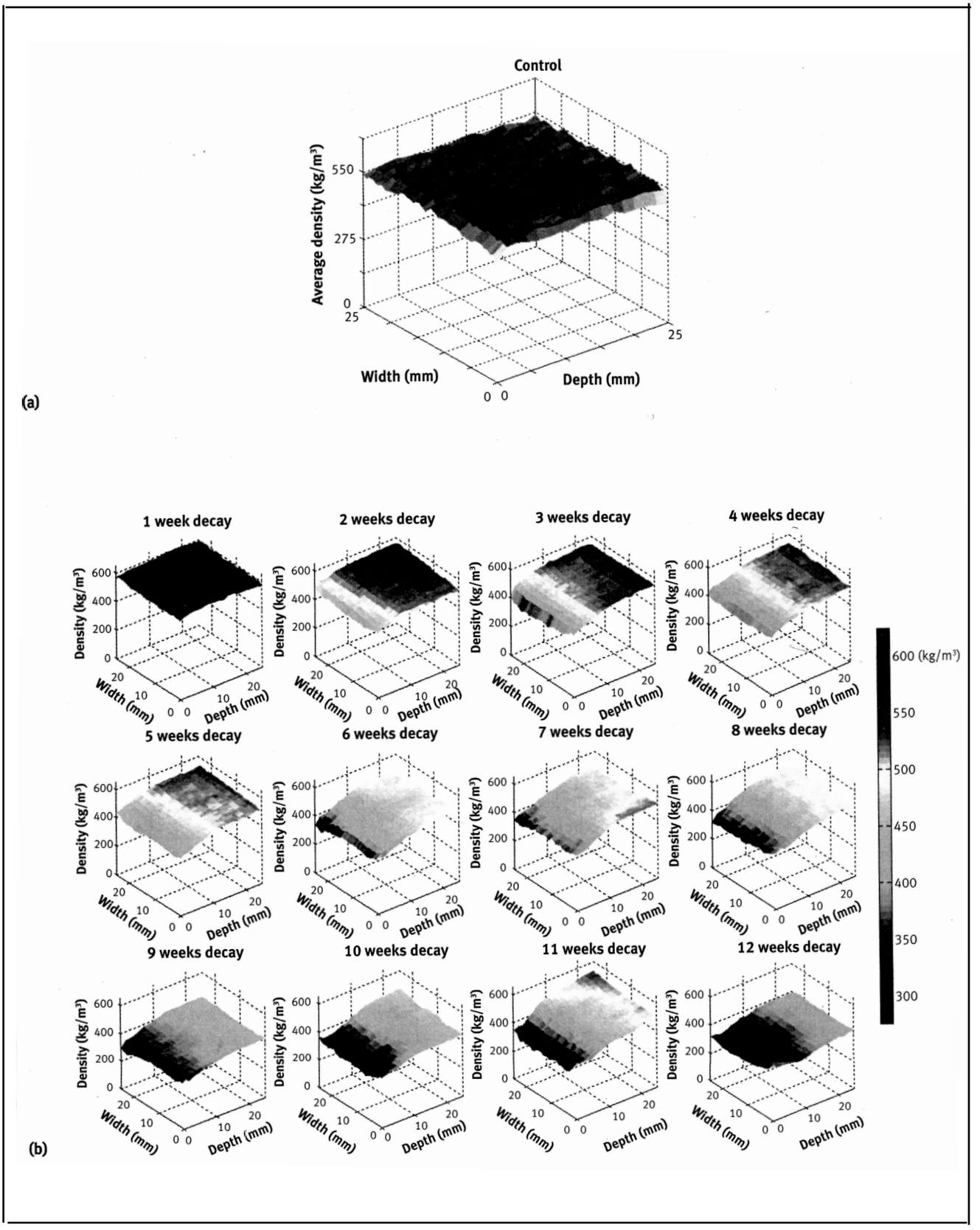

Figure 3. Density of decayed blocks: (a) averaged density for the control blocks (the average was performed along the height for the control blocks); and (b) densities averaged along height for blocks decayed from one week to 12 weeks.

weeks of exposure to decay, where week 12 had the most loss. As illustrated in Figure 2a, the mass loss results indicate that considerable mass loss can be associated with increased exposure to wood-destroying fungi (or increased decay). Similarly, as illustrated in Figure 2b, the volume calculations confirm that a volume loss is associated with increased decay.

The average densities of the wooden blocks (averaged along the height dimension, see Figure 1) were computed and plotted. Figure 3a shows this average density for the control blocks. Figure 3b shows this average density for blocks exposed to control decay from 1 to 12 weeks. These plots make it easy to see how the blocks experienced the most density loss at the face in contact with the fungi and how the level of decay (that is, mass loss) decreased progressively towards the opposite face. In Figure 3b the blocks subjected to only one week of decay seem to have experienced minimal to no density loss on the surface not in contact with the fungi; the average density value at this point was approximately 600 kg/m^3. At the surface in contact with the fungi, blocks with one week of decay had an average density of approximately 570 kg/m^3; thus, they seem to have experienced a relatively small density loss at the surface in contact with the fungi. These results indicate that decay can be detected by X-ray computed tomography as early as one week based on the relative density change. In contrast, Figure 3b also shows that specimens with 12 weeks of exposure to fungi experienced a density loss throughout the entire block with average densities ranging from 275 kg/m^3 at the surface in contact with fungi to 400 kg/m^3 at the opposite face.

Figures 4a and 4b show the average densities of the wooden blocks along cross-sectional areas normalized using the average density of the control blocks. These average density values were plotted versus the specimen's depth (Figure 1), and two different plots are shown for viewing simplicity. Please note that specimens exposed to decay for only one week had a higher mass post-decay than the control block; thus, the density was higher, perhaps caused by moisture absorption. For this reason, a dotted line was drawn, which depicts week 1 translated so that the maximum values coincide with the values associated with the control blocks. This allows the observation that there is a small measurable density loss at the surface in contact with the fungi when exposed for one week of controlled decay.

The percent density loss versus depth (Figure 1c) is plotted in Figure 4c. These results indicate that noticeable density loss occurred from decay in a relatively short period of time (that is, one week). Note how specimens exposed to 12 weeks of decay lost 47% of their density at the face in contact with the fungi and experienced only a 28% loss on the opposite face. Conversely, specimens with one week of decay appear to have experienced only a 5% density loss on their most decayed face. Again, the dotted line in Figure 4c depicts a translated line for specimens with one week of decay so that their minimum values coincide with the values associated with the control specimens.

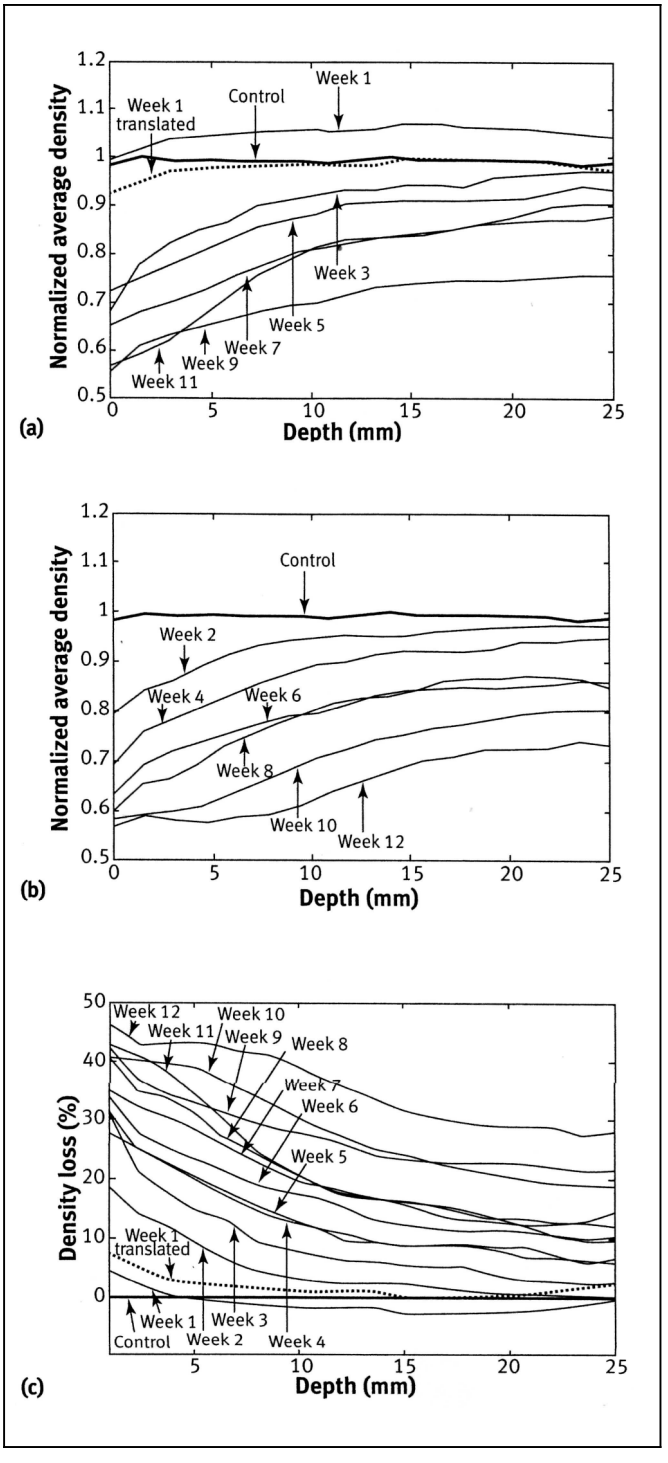

Figure 4. Percentage density loss of decayed blocks: (a) densities averaged along height and width and normalized to the average of the control density for blocks decayed 1, 3, 5, 7, 9 and 11 weeks, (b) densities averaged along height and width and normalized to the average of the control density for blocks decayed 2, 4, 6, 8, 10 and 12 weeks; and (c) percentage of mass density loss plotted along the depth for all blocks subjected to controlled decay. The dotted line represents the results for specimens exposed to one week of controlled decay translated so that its maximum values are equivalent to the average density of the control blocks.

Ultrasonic Measurements

As shown in Figure 1, the wooden cubes had a multilayered structure and, therefore, may be dispersive at relatively higher frequencies when the wavelength is on the same order of magnitude as the dimensions of the cube/growth ring thickness. Also, the latewood and earlywood had different densities and material properties, where the density and velocities for latewood are typically higher than those of earlywood (Bucur, 2006; Bucur and Archer, 1984; Bodig and Jayne, 2003). Figure 1 b shows the three principal material directions and associated velocities, including the different polarization of the shear waves. During the controlled decay process, the wooden specimens with a nominal dimension of 25.4 mm had a non-uniform volume reduction. For example, the specimens exposed to 12 weeks of decay had a volume loss of ~30% and the smallest cross-section dimension measured was approximately 14.5 mm. This change in dimension is illustrated in Figure 1c. Figure 1c also shows that the initially parallel wooden cube faces were distorted after exposure to decay. Because of a lack of parallel surfaces in the decayed wooden cubes, the cubes were sanded to restore parallel reflective surfaces. The sanding process was carefully done because of the fragile nature of the decayed cubes. Care was also taken to keep the wooden specimens at a constant relative humidity of 30% and at a room temperature of approximately 300 K (27 °C).

Contact ultrasonic transducers with a center frequency of 100 kHz were used, with the longitudinal and shear transducers having an element diameter of 38.1 and 25.4 mm, respectively. Vacuum grease was used as an ultrasonic couplant, because the transmission losses were relatively low (Bucur, 2006; Bucur and Archer, 1984). However, wood can absorb couplant over time because it is porous. To validate its use, couplant was applied excessively to wood specimens, and velocity measurements were taken over a period of an hour. No significant variability in the velocity was observed during the one-hour period. However, after a three-day period, the longitudinal velocity was estimated to be nearly 1000 m/s higher than the velocity measured when the couplant was applied. Should many tests need to be performed, cellophane (which closely matches the wood acoustic impedance) can be placed between the couplant and the specimen (Bucur, 2006; Bucur and Archer, 1984). Dry couplant cannot be used in these measurements because it requires the application of excessive pressure, which may damage the more decayed (that is, fragile) wooden cubes.

A ~0.91 m long steel rod (to separate out the successive echoes) with a diameter of 25.4 mm was used as a delay line during ultrasonic longitudinal velocity and attenuation measurements. Several authors presented a pulse-echo technique for thin specimens where back-wall echoes can be separated by coupling a buffer rod to the specimen to delay the signal, and therefore separate out the back-wall echoes (McSkimin, 1950; Papadakis, 1968). By using a buffer rod, the transmitted waveform will be fully formed before it propagates through the specimen. In addition to its small material attenuation, the steel rod also allows for the signal loss at the steel/wood boundary to be characterized, which is a requirement for the attenuation measurements in the wooden specimens. Figure Sa shows the energy velocity dispersion curves for the steel rod used in this study (Pavlakovic and Lowe, 2001; Rose, 1999). For the shear wave velocities and corresponding attenuation measurements, a steel plate with a thickness of ~63.5 mm was used as a delay line to stabilize the ultrasonic beam.

Figure 5b shows a single pulse transmitted through a steel rod that was coupled to a wooden specimen. The solid lines represent the echoes that were detected (echoes 1 and 2) by the receiving transducer, while the dashed lines represent possible echoes that were not detected (echoes 3 and 4) because of the large reflection coefficient between steel and wood and the high attenuation coefficient of wood. The amplitudes of the received echoes can be written as:

$$A_1 = A_T T_L T_R T_{sw} \exp(-\alpha_s d_s)\exp(-\alpha_w d_w) \tag{1}$$

$$A_2 = A_T T_L R_L T_R R_{sw} T_{sw} \exp(-3\alpha_s d_s)\exp(-\alpha_w d_w) = A_1 R_{sw} R_L \exp(-2\alpha_s d_s) \tag{2}$$

where

T_{sw}, T_L, T_R, R_{sw}, R_L and R_R are the transmission and reflection coefficients, as denoted in Figure 5b,
d_s is the length of the steel buffer rod,
a_s is the attenuation coefficient of steel due to mode conversion and scattering,
a_w is the attenuation coefficient of wood.

The subscripts *w* and *s* correspond to values for wood and steel, respectively. Measurements were also taken using only the steel rod for reference purposes. The values of A_T and A_R (or A_R^*) represent the amplitudes of the transmitted and received signal, respectively. The amplitudes of the received echoes (see Figure 5c) can be written as follows:

$$A_1^* = A_T T_L T_R^* \exp(-\alpha_s d_s) \tag{3}$$

$$A_2^* = A_T T_L R_R^* R_L T_R^* \exp(-3\alpha_s d_s) = A_1^* R_R^* R_L \exp(-2\alpha_s d_s) \tag{4}$$

where

all variables have been defined previously.

The transmission and reflection coefficients are depicted in Figure 5c. Note that the transmission and reflection coefficients on the transmitting side will not change between the

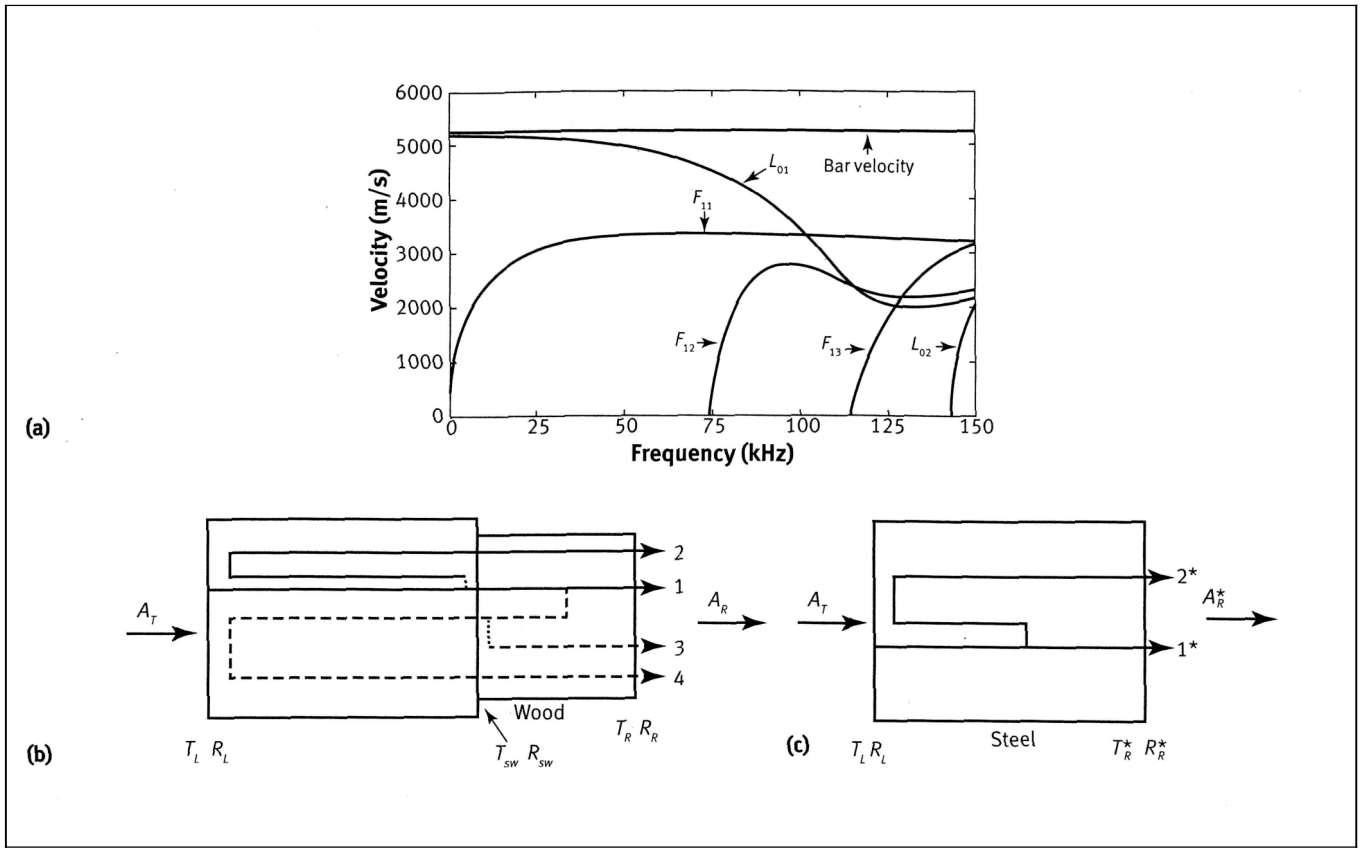

Figure 5. Ray path analysis for acoustic measurements: (a) group velocity dispersion curve for steel buffer rod with labeled guided wave modes; and (b) steel rod and wooden specimen showing possible echoes at different interfaces (the dashed lines represent possible echoes that were not detected; the solid lines represent detected echoes where A_T and A_R represent the transmitted and received signals, respectively); and (c) steel rod alone where A_T and A_R^* represent the transmitted and received signals, respectively.

setups containing the wood specimens and the setups containing only the steel.

The amplitude reflection coefficient is theoretically described by the following equations:

$$R_{sw} = \frac{z_w - z_s}{z_w + z_s} \tag{5}$$

$$z = \rho c \tag{6}$$

where

z is the characteristic acoustic impedance,
c is the bulk wave velocity,
ρ is the density of the respective medium (Kinsler et al., 1980).

The order of s and w in the subscripts on the reflection and transmission coefficients describe the order of the interface of the two media relative to the signal propagation. For example, if the subscript is *sw*, then the signal is transmitted from the steel to wood and vice versa. The order of the media is important due to phase. Switching the order of the media will yield a reflection coefficient that is 180° out of phase from the original, thus resulting in Equation 7.

$$|R_{sw}| = |-R_{ws}| \tag{7}$$

However,

$$|T_{sw}| \neq |-T_{ws}| \tag{8}$$

All reflection coefficients are related to the transmission coefficient at a similar boundary by the following equation.

$$R = T - 1 \tag{9}$$

Theoretically, the characteristic acoustic impedances for steel and sound wood in the longitudinal direction are 39 Pa × s/m and 1.57 Pa × s/m, respectively. This yields an

energy reflection coefficient of0.85. Thus, 8.5% ofthe energy ofthe transmitted wave will be reflected back, and only 15% of the energy will be transmitted through the wooden cubes. Furthermore, there will be a loss at the interface due to the imperfect coupling between the steel and wood, so it is necessary to characterize the actual reflection coefficient. The actual reflection coefficient at the steel/wood interface can be calculated by looking at Equations 1 and 2, which correspond to echoes 1 and 2. The reflection coefficient at the steel/wood interface can be found by the following equation, where R_L (see Figures 5b and 5c) is the reflection coefficient at the side where the signal is transmitted.

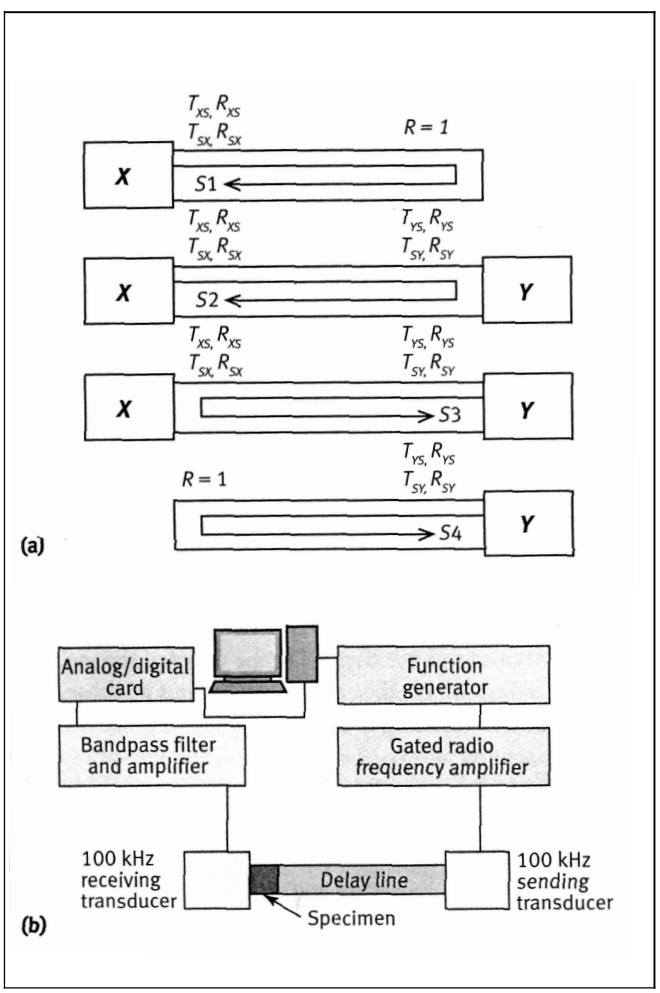

Figure 6. Experimental setup: (a) technique for finding reflection coefficients at steel rod/transducer boundaries for corrections in steel attenuation Coefficient measurements (both the X and Y sensors can serve as sending and receiving transducers); and (b) schematic diagram of experimental setup. A steel rod 0.91 m long and 25.4 mm in diameter was used as a delay line for longitudinal velocity and attenuation measurements. A steel plate 63.5 mm thick was used as a delay line for shear velocity and attenuation measurements.

$$R_{sw} = \left(\frac{A_2}{A_1}\right)\left(\frac{\exp(2\alpha_S)}{R_L}\right) \quad (10)$$

The reflective surface, R_L, should not be approximated as a free surface (R_L = 1), because some ofthe wave will be transmitted to the receiver and signal loss via the couplant will occur. A switching technique can be used to approximate the unknown reflection coefficients, as shown in Figure 6a (Kim et al., 2009). First, the transducer, X, is coupled to one side of the steel bar and operated in a pulse-echo configuration (see the first part of Figure 6a). The amplitude ofthe first received signal, A_{S1}, can be written as:

$$A_{S1} = A_T T_{XS} T_{SX} \exp(-2\alpha_s d_s) \quad (11)$$

where

A_s is the amplitude ofthe transmitted signal.

Now, the other transducer, *Y*, is coupled to the opposite end ofthe steel rod (see the second part of Figure 6a), while transducer X still operates in pulse-echo mode. The amplitude ofthe first received signal, A_{S2}, can then be written as Equation 12.

$$A_{S2} = A_T T_{XS} T_{SX} R_{SY} \exp(-2\alpha_s d_s) \quad (12)$$

Next, transducer Y is configured to operate in pulse-echo mode (see the third part of Figure 6a). This is done without changing the setup. The amplitude ofthe first received signal, A_{S3}, can be written as:

$$A_{S3} = A_T^* T_{YS} T_{SY} R_{SX} \exp(-2\alpha_s d_s) \quad (13)$$

where

A_T^* is the amplitude ofthe transmitted signal.

Finally, transducer X is removed without disturbing the coupling between transducer Y and the steel rod, while transducer *Y* is still operating in pulse-echo configuration (see the fourth part of Figure 6a). The amplitude ofthe first received, A_{S4}, signal can be written as Equation 14.

$$A_{S4} = A_T^* T_{YS} T_{SY} \exp(-2\alpha_s d_s) \quad (14)$$

Noting that the X and Y sensors are nominally the same sensors, R_L and R_R* (see the fourth part Figure 6a) can be foundasfollows.

$$R_R^* = R_{SY} = \frac{A_{S2}}{A_{S1}} \quad (15)$$

$$R_L = R_{SX} = \frac{A_{S3}}{A_{S4}} \quad (16)$$

The values of R_L and R_R^* will be necessary when calculating the attenuation coefficient of steel. The reflection coefficient at the steel/wood interface is high (very close to 1); thus, the portion of the signal that traverses both the steel and specimen three times (see echo 4 in Figure 5b) is too small in amplitude to detect. The R_R value will be approximated as $-R_{sw}$ because the acoustic impedance of the transducer face nearly matches that of the steel rod.

Velocity and Attenuation Measurements

Figure 6b shows a schematic diagram of the ultrasonic measuring system. As illustrated in Figure 6b, a function generator was used to generate a 100 kHz square pulse. The pulse was amplified with a gated radio frequency amplifier and sent to the sending transducer. Both the sending and receiving transducers had a center frequency of 100 kHz. The average of 16 waveforms (in order to maximize the signal-to-noise ratio) was recorded after being digitized using a sampling frequency of 3.125 MHz.

Velocity Measurements

Velocity measurement techniques are reviewed in outside work (McGovern, 2011). Because of the multilayered nature of the wood specimens, the ultrasonic pulse may not maintain its original shape because of dispersion (Pavlakovic and Lowe, 2001; Rose, 1999). For this reason, the phase-comparison technique for calculating arrival time is advantageous (Sachse and Pao, 1978). First, a pulse is transmitted through the steel delay line alone. Next, a pulse is transmitted through the steel/specimen setup, as depicted in Figure 5b. Because of the multilayered nature of the wooden specimens, the velocity measurement of the wood specimens is the energy velocity of the fastest mode. The angle of the fast fourier transform is computed from the signals to find the phase. The phase is unwrapped to account for jumps equal to or greater than 180". The phase velocity can then be obtained from the following equation:

$$v(f) = \frac{2\pi \times f \times d_w}{\left(\phi_w(f) - \phi_s(f)\right)} \tag{17}$$

where

ϕ_w denotes the phase for the signal passed through the wood/steel setup,
ϕ_s denotes the phase of the signal obtained from just the steel delay line,
d_w is the distance traveled through the wood,
f is the frequency.

Only the linear portions of the phase spectrum are used to calculate velocity.

Attenuation Measurements

First, a pulse is transmitted through steel alone. Next, a pulse is transmitted through the steel/specimen setup, as depicted in Figure 5b. A first-order, narrow-band (1 kHz) Butterworth filter is applied to the signal received from the steel/specimen setup at each desired frequency band. This sliding narrow-band filter is also applied to the signal received from the steel reference medium. The attenuation coefficient, a_w, for the wooden cube can be found by dividing Equation 1 by Equation 3 to yield the following:

$$\alpha_w(f) = \frac{-1}{d_w}\left[\ln\left(\left|\frac{A_1(f)}{A_1^*(f)}\right|\right) - \ln\left(\left|T_{sw}(f)\right|\right) - \ln\left(\left|\frac{T_R(f)}{T_R^*(f)}\right|\right)\right] \tag{18}$$

where

all terms have been previously defined.

The values of T_R, T_R^* and T_{sw} can be found as described previously. Note that T_{sw} is a function of the attenuation coefficient of steel. The attenuation coefficient of steel can be found by dividing Equation 3 by Equation 4 and is described by the following equation:

$$\alpha_{\text{steel}}(f) = \frac{-1}{2d_s}\left[\ln\left(\left|\frac{A_2^*(f)}{A_1^*(f)}\right|\right) - \ln\left(\left|R_R^*(f)R_L(f)\right|\right)\right] \tag{19}$$

where

all terms have also been previously defined.

Results from Ultrasonic Measurements

Experimental velocity and attenuation measurements were taken in the longitudinal, radial and tangential directions for all specimens using longitudinal and shear transducers centered at 100 kHz. The velocities measured were v_{LL}, v_{LR}, v_{LT}, v_{RR}, v_{RL}, v_{RT}, v_{TT}, v_{TL} and v_{TR}, where the first subscript denotes the ultrasonic wave energy direction of propagation, and the second subscript denotes the wave polarization (see Figure 1b). Similarly, the magnitudes of the corresponding attenuation coefficients were also measured: α_{LL}, α_{LR}, α_{LT}, α_{RR}, α_{RL}, α_{RT}, α_{TT}, α_{TL} and α_{TR}. In an attempt to minimize error introduced during measurements, a minimum of five independent ultrasonic tests was carried out for all nine measurements for each of the 70 wooden blocks. The broadest possible frequency bandwidth (up to 200 kHz) of the velocity and attenuation data depended upon the operating range of the transducers and attenuation of the specimens. Above 200 kHz, it was difficult to obtain a signal through some orientations of the more decayed specimens because of low signal-to-noise

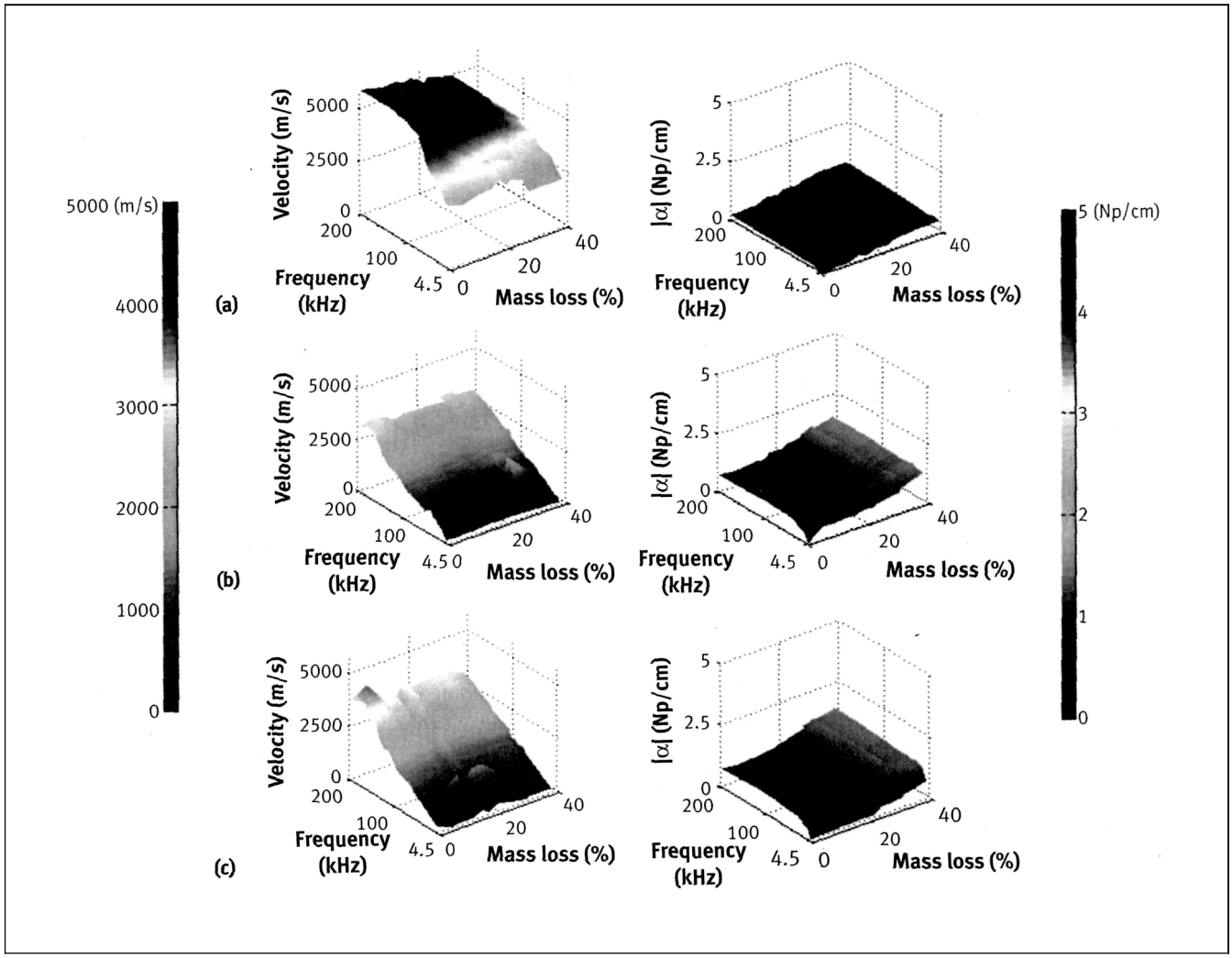

Figure 7. Experimentally obtained velocities (left column) and attenuations (right column) for ultrasonic waves propagating in the longitudinal direction polarized in the: (a) longitudinal; (b) radial; and (c) tangential direction as a function of frequency and mass loss during exposure to controlled decay. The variability shown in the raw data is due to the natural variability of the wood including different growth ring thicknesses and lack of perfect parallelism of the growth rings to the faces of the wooden cube specimens.

ratio (due to high material attenuation). Additionally, waveform distortion poses problems when using the phase-comparison technique, which leads to a reduction of bandwidth. Waveform distortion is mainly caused by the multilayered nature of the wooden specimens, which leads to guided wave effects at higher frequencies (earlywood and latewood material properties are different from each other), or to the strong increase of attenuation with increasing frequency and amount of decay.

The velocity and attenuation measurements associated with the longitudinal principal material direction are presented in Figure 7 as a function of mass loss and frequency. The variability observed in Figure 7 is acceptable, particularly when considering the variation in growth ring thickness, which may lead to a different number of rings for each wooden cube, and when considering that the rings are only nearly parallel to the surface of the wooden cubes. Because of space limitations, the velocity and attenuation plots corresponding to the other two principal material directions, that is, radial and tangential, are not shown. Polynomial surfaces were fitted to the experimentally obtained plots (with the decay measured in percent mass loss rather than weeks subjected to controlled decay) using a least squares fitting technique (MATLAB, 2010). This is acceptable because the percent mass loss is linearly related to the number of weeks subjected to decay (McGovern, 2011). Figures 8, 9 and 10 show the polynomial surface fits, where the left and right columns represent the velocity measurements and the magnitude of the corresponding attenuation coefficient measurements, respectively.

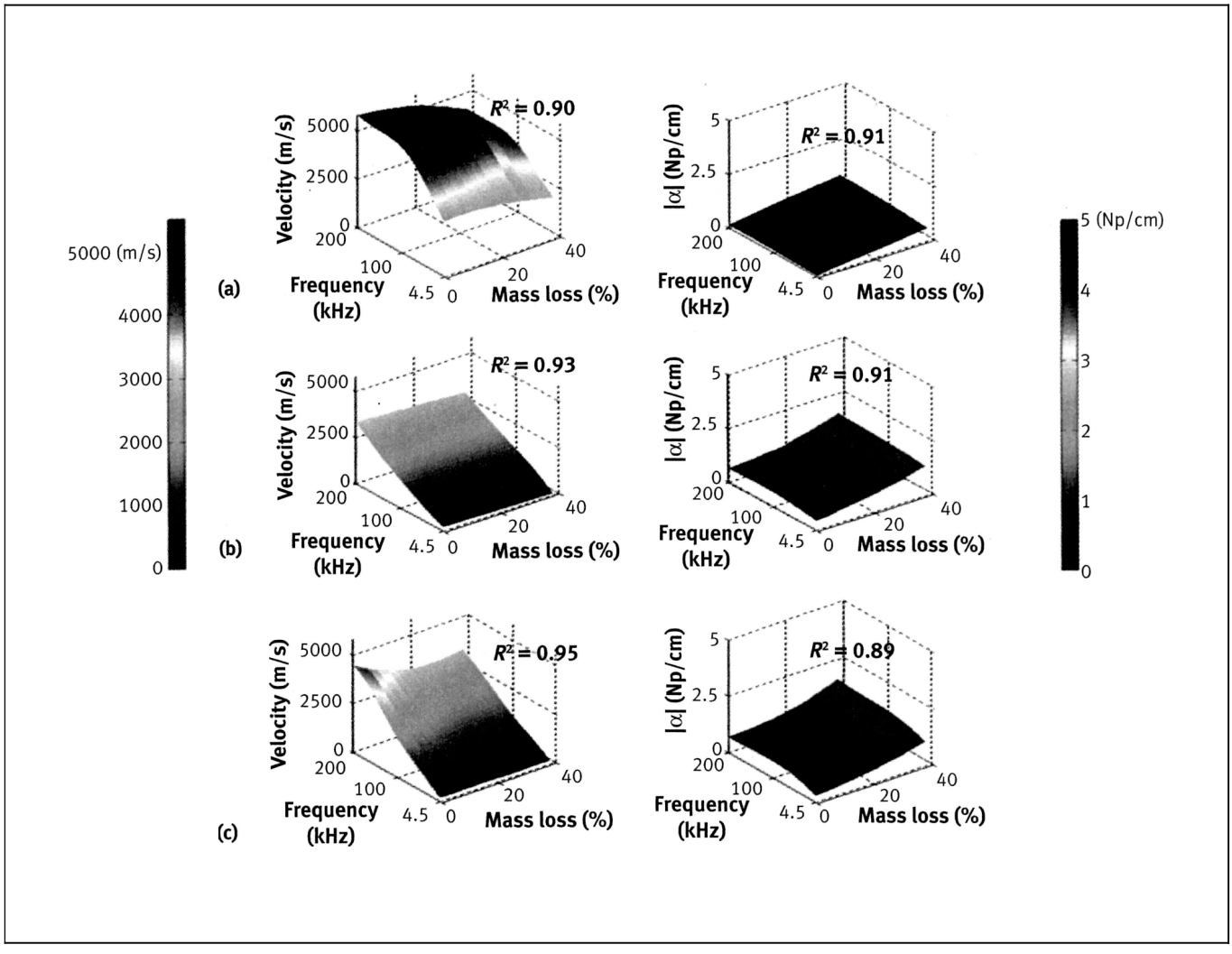

Figure 8. Velocities (left column) and attenuations (right column) for ultrasonic waves propagating in the longitudinal direction polarized in the: (a) longitudinal; (b) radial; and (c) tangential direction fitted to polynomials a function of frequency and mass loss during exposure to controlled decay. R^2 values are presented as a measure of goodness of fit of the polynomial to actual data.

Tables 1 to 3 show the coefficients for the various polynomial fits for the velocities and the corresponding attenuations, respectively, as a function of frequency and percent mass loss associated with the three principal material directions. The greatest discrepancies between the polynomial surface fits and the experimentally obtained data lie with specimens submitted to 11 weeks of controlled decay. Data associated with week 11 did not seem to fit with any trends, including the velocity, attenuation and percentage of mass loss. This could potentially be explained by the relative environmental location of the specimens during the decay process. The surfaces shown in Figures 8 to 10 match the corresponding experimental data quite closely. For each case, the corresponding R^2 is also shown. At the extents of the frequency bandwidths, the polynomial fits for the velocity measurements became difficult to constrain at the edges. To overcome the difficulty posed in constraining the edges, the velocity surfaces were split up into two regimes: acoustic (see Table 2) and ultrasonic (see Table 3) range. The polynomial surface fits matched the actual data quite closely; the percent difference between the measured data and the fitted surface did not exceed 15% (at the edges of the surface area) and for most cases stayed significantly below 10% (in the center of the surface area). The measured ultrasonic velocity and attenuation values presented here represent the energy velocity and attenuation values of the fastest wave mode. Furthermore, because within each test specimen, there were variations in velocity and attenuation, the reported measurements do not represent values at a point; rather they represent velocity and attenuation values averaged over the specimen dimensions.

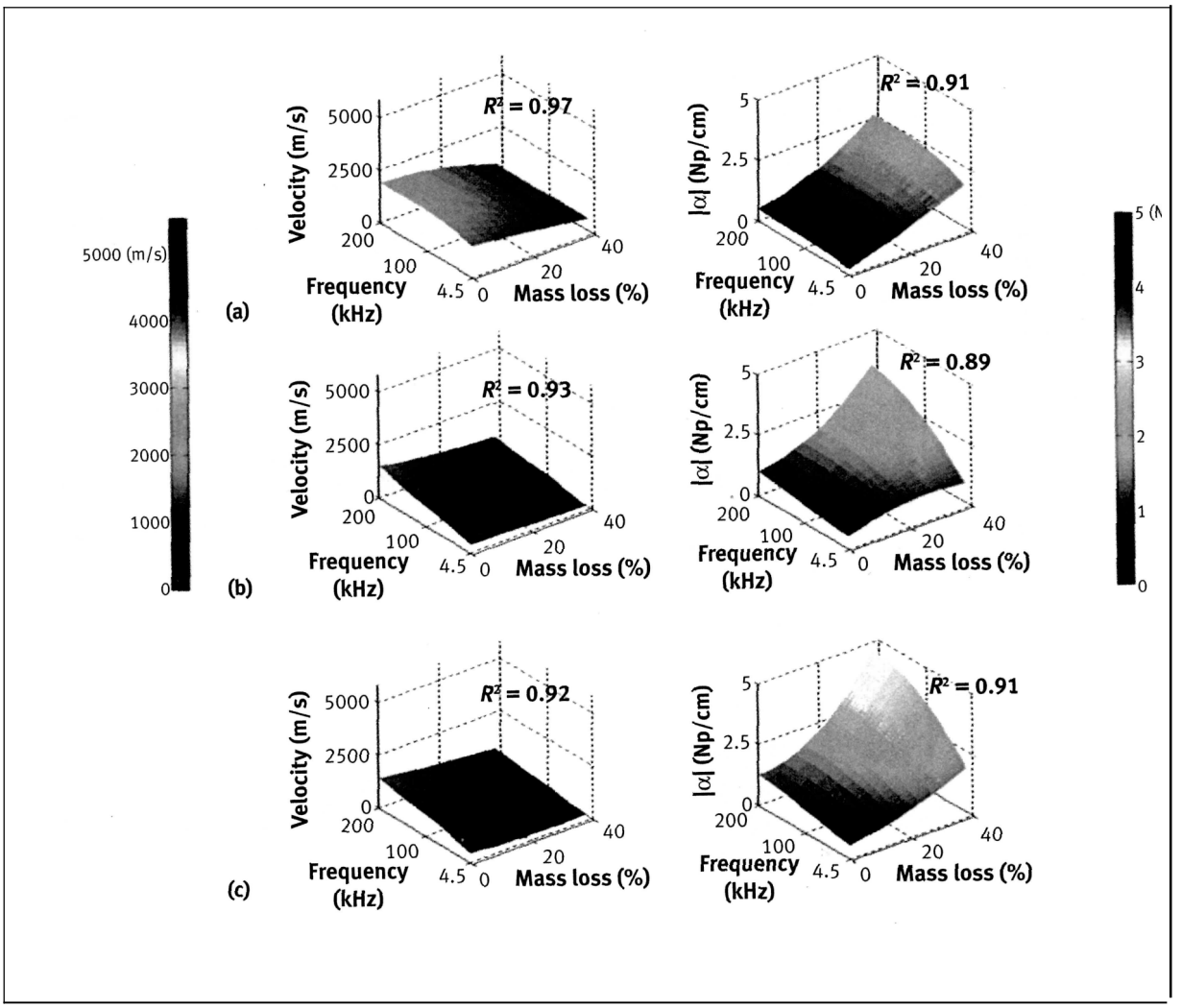

Figure 9. Velocities (left column) and attenuations (right column) for ultrasonic waves propagating in the radial direction polarized in the: (a) radial; (b) longitudinal; and (c) tangential direction fitted to polynomials a function of frequency and mass loss during exposure to controlled decay. R^2 values are presented as a measure of goodness of fit of the polynomial to actual data.

TABLE 1

Polynomial fits for attenuation coefficients as a function of frequency and percent mass loss (up to 40%) for the three principal material directions and three different wave polarizations for a frequency range of 4.5 to 200 kHz

$$\alpha(x,y) = A_\alpha + B_\alpha x + C_\alpha y + D_\alpha x^2 + E_\alpha xy + F_\alpha y^2 + G_\alpha x^2 y + H_\alpha xy^2 + I_\alpha y^3 *$$

Coefficient	Principal material direction – polarization direction								
	LL	*LR*	*LT*	*RR*	*RL*	*RT*	*TT*	*TL*	*TR*
A_α	0.45937	0.93749	0.93989	1.31110	1.64566	1.93714	1.27111	1.66975	1.76142
B_α	0.17677	0.22694	0.20719	0.60610	0.58013	0.85167	0.42770	0.40410	0.44761
C_α	0.05638	0.01021	−0.01041	0.03540	0.22686	0.32096	0.11495	0.31784	0.32387
D_α	−0.00363	0.05056	0.05968	0.07174	0.05055	0.17319	0.07736	0.02911	0.13941
E_α	0.01073	0.00355	0.01157	0.03467	0.17461	0.15555	0.02009	0.11523	0.06093
F_α	−0.01161	−0.02839	−0.06810	−0.06143	−0.08166	−0.11495	−0.07227	−0.09389	−0.10422
G_α	−0.00252	0.00756	0.01017	0.02375	0.07800	0.05875	−0.00352	0.01604	0.00716
H_α	−0.00253	0.00967	0.00803	-0.02354	−0.0498	−0.05808	−0.01576	−0.04268	−0.02528
I_α	−0.00160	0.00681	0.03601	0.00622	−0.01124	−0.01124	0.00194	−0.01086	−0.01965

* *Values are centered* by the mean and scaled by the standard deviation; x = (mass loss [%] − μ_m) / σ_m, where μ_m = 19% and σ_m = 10.6%; y = (frequency [Hz] − μ_{freq}) / σ_{freq}, where μ_{freq} = 102 000 Hz and σ_{freq} = 56 580 Hz.

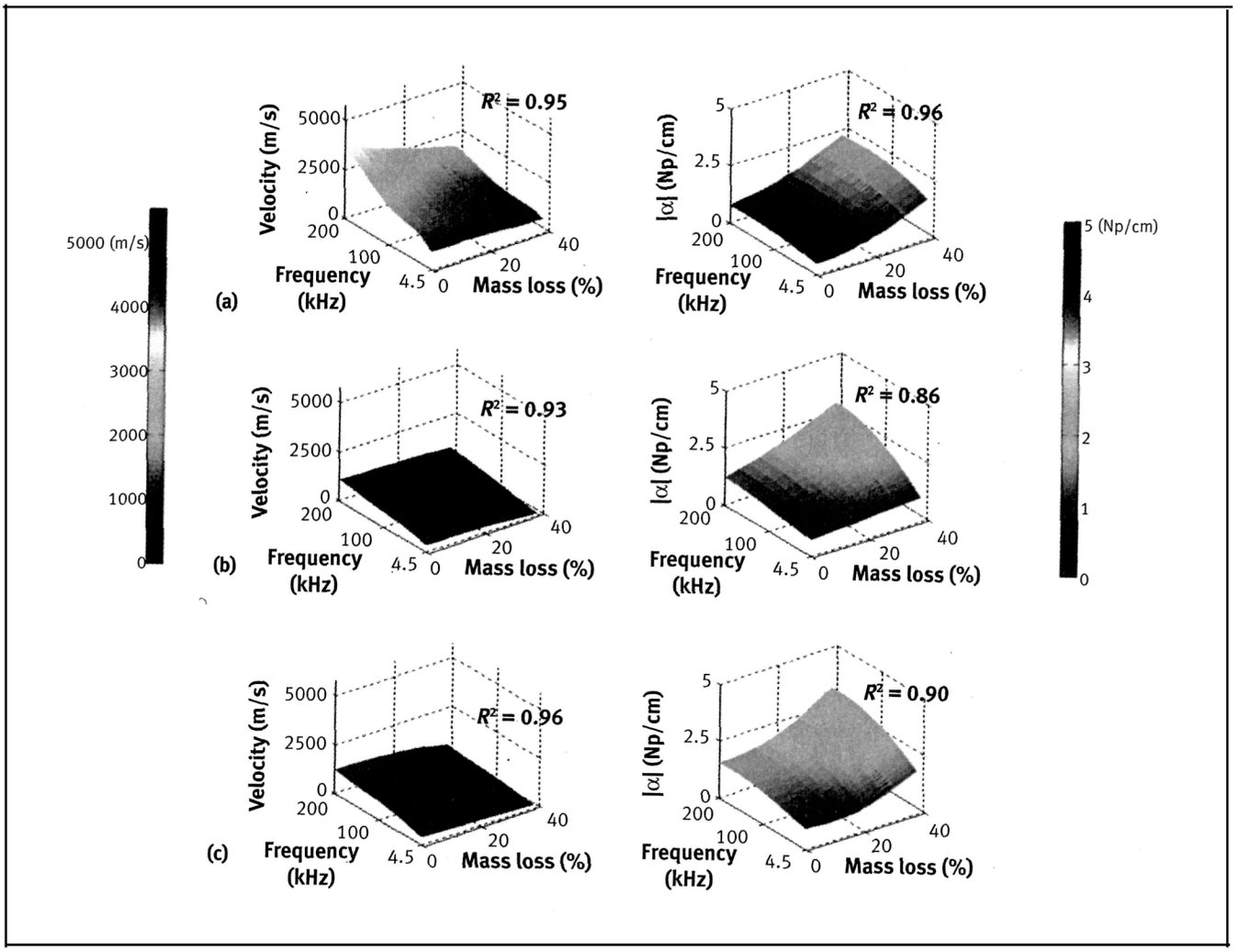

Figure 10. Velocities (left column) and attenuations (right column) for ultrasonic waves propagating in the tangential direction polarized in the: (a) tangential; (b) longitudinal: and (c) radial direction fitted to polynomials as a function of frequency and mass loss during exposure to controlled decay. R^2 values are presented as a measure of goodness of fit of the polynomial to actual data.

TABLE 2
Polynomial fits for velocity coefficients as a function of frequency and percent mass loss (up to 40%) for the three principal material directions and three different wave polarizations for a frequency range of 4.5 to 20 kHz

$$V(x,y) = A_V + B_V x + C_V y + D_V x^2 + E_V xy + F_V y^2 *$$

Coefficient	Principal material direction – polarization direction								
	LL	*LR*	*L–T*	*RR*	*RL*	*RT*	*TT*	*TL*	*TR*
A_V	2920	291.8	369.2	1225	357.9	327.1	1009	359.5	341.2
B_V	−240.6	−28.12	−7.307	−194.5	−53.20	−52.94	−85.74	−71.19	−59.01
C_V	118.7	75.71	97.72	25.48	29.44	26.99	74.91	24.51	20.09
D_V	−71.18	4.614	0	−12.20	4.206	23.81	−12.21	−27.80	−0.959
E_V	−12.67	10.26	0	−6.759	−2.996	−5.360	−12.40	−2.307	−3.843
F_V	0.394	−0.564	0	−0.607	−0.159	−0.083	−4.273	−0.173	−0.069

* Values are centered by the mean and scaled by the standard deviation; x = (mass loss [%] − μ_m) / σ_m, where μ_m = 19% and σ_m = 10.6%; y = (frequency [Hz] − μ_{freq}) / σ_{freq}, where μ_{freq} = 12 000 Hz and σ_{freq} = 4611 Hz.

TABLE 3
Polynomial fits for velocity coefficients as a function of frequency and percent mass loss (up to 40%) for the three principal material directions and three different wave polarizations for a frequency range of 20 to 200 kHz

$$V(x,y) = G_V + H_V x + I_V y + J_V x^2 + K_V xy + L_V y^2 + M_V x^2 y + N_V xy^2 + O_V y^3 + P_V x^2 y^2 + Q_V xy^3 + R_V y^4 + S_V x^2 y^3 + T_V xy^4 + U_V y^5 *$$

Coefficient	Principal material direction – polarization direction								
	LL	LR	LT	RR	RL	RT	TT	TL	TR
G_V	5048	1591	1632	1550	782.9	756.7	1498	720.0	695.1
H_V	−422.3	4.779	−123.5	−301.7	−82.73	−119.0	−242.8	−74.88	−125.7
I_V	750.8	809.8	790.9	65.74	101.2	116.7	386.5	125.2	180.9
J_V	−105.6	0	76.25	−59.04	1.717	16.92	6.882	−22.77	1.890
K_V	−32.40	−54.68	−132.1	−26.58	−29.78	−8.011	−109.1	18.02	−19.21
L_V	−623.0	32.76	225.7	−60.60	−44.23	−60.99	308.2	−27.40	−14.20
M_V	−52.11	0	125.5	−19.23	19.92	7.940	34.25	9.874	−24.11
N_V	45.22	−12.11	−42.19	34.97	−22.51	6.575	−49.61	1.769	16.31
O_V	90.74	23.51	8.666	33.33	102.6	95.13	−27.63	60.89	52.43
P_V	3.542	0	2.007	8.422	7.136	3.131	0.326	1.938	−11.62
Q_V	−15.97	15.84	12.69	−2.170	−2.270	−10.91	−9.912	−5.452	−3.800
R_V	106.6	−5.083	−72.47	0.790	8.496	14.49	−85.20	3.676	8.766
S_V	14.94	0	−22.99	−0.036	−6.117	−4.312	−5.750	−2.251	4.160
T_V	−4.758	−6.053	11.13	−4.502	5.179	0.568	12.92	1.661	−2.544
U_V	−39.33	−0.566	14.11	−4.517	−20.03	−20.52	29.20	−12.41	−13.64

* Values are centered by the mean and scaled by the standard deviation; x = (mass loss [%] − μ_m) / σ_m, where μ_m = 19% and σ_m = 10.6%; y = (frequency [Hz] − μ_{freq}) / σ_{freq}, where μ_{freq} = 100 100 Hz and σ_{freq} = 56 580 Hz.

Figures 4a, 4b and 4c indicate that the presence of decay does not lead to a reflective interface between sound and decayed wood in the traditional sense; instead, there is a continuous variation (that is, gradation) of the acoustic impedance values from those associated with sound wood to those associated to decayed wood. Wave propagation between two materials separated by a graded material layer of finite thickness has already been studied, where the authors have shown that, for normal incidence, the level of energy transmitted/reflected by the graded interface depends upon the ratio of the wavelength to the interface graded material layer thickness (Aebi et al., 2007; Chiu and Erdogen, 1999; Vollmann et al., 2006). If the wavelength of a normal incident wave is small relative to the thickness of the graded interface, reflections will occur; however, if the wavelength is relatively large, the incident wave will be transmitted with minimal reflections. For a wave propagating parallel to the graded region, dispersion will occur. Furthermore, the boundaries between sound and decayed wood (that is, graded interface) are typically irregular, resembling more a saw-tooth profile than a plane surface. Wave propagation across an interface having a saw-tooth profile has also been studied (Proud and Tamarkin, 1957). Given the high attenuation values of decayed wood and the lack of a perfect reflective interface between sound and decayed wood, decayed wood behaves as an energy sink; that is, no energy is reflected back from a probing ultrasonic beam. This phenomenon has been experimentally observed by others (Beall et al., 1994; Senalik et al., 2010; Titta et al., 1998). Considering the material properties variability and the anisotropy inherent in wood products, these phenomena contribute to make the ultrasonic detection and assessment of wood decay a difficult task (Bucur, 2006; Bucur and Archer, 1984).

Conclusion

Seventy wooden block cubes made of loblolly pine wood *(P. taeda)* were prepared following ASTM standards and exposed to fungus *(G. trabeum)* for different, known periods of time up to 12 weeks. X-ray computed tomography was carried out. It was verified that the most decay occurred at the face in contact with the fungus and that the decay level decreased towards the opposite face. It was also observed that a considerable decrease in volume and mass occurred with increasing exposure to decay. Blocks decayed for 12 weeks experienced the most average mass loss (~40%), average volume loss (—30%) and average density loss (—35%). Specimens exposed to only one week of controlled decay also exhibited some loss in density (—5%); however, the mass loss was difficult to evaluate due to initial moisture absorption. These results indicate that, based on the relative density change, wood decay can be detected using X-ray tomography as early as one week The non-uniformity in decay through the thickness was also quantified. Blocks subjected to controlled decay for 12 weeks lost 47% of density at the

surface in contact with the fungus and 28% at the opposite surface, while blocks subjected to only one week of decay experienced 5% density loss at the surface in contact with the fungi and nearly 0% at the opposite surface. Results also indicate that the presence of decay led to a continuous variation of acoustic impedance (that is, a graded layer interface) and not to the creation of a perfect acoustic reflective interface between sound and decayed wood. This lack of a well-defined reflective surface separating sound from decayed wood explains some of the difficulties encountered in detecting and assessing decay using traditional linear acoustic/ultrasonic techniques.

Ultrasonic velocity and attenuation measurements were also carried out using the same wood specimens with controlled amounts of decay for the frequency band of 4.5 to 200 kHz. For each of the material principal directions, both velocity and attenuation values were found to be dependent upon frequency and amount of decay, that is, percentage of mass loss. It was observed that velocity increased with increasing frequency and decreased with increasing amount of decay, while attenuation increased with increasing frequency and decay. For example, for the control blocks with no decay, the energy velocity of the fastest mode through the longitudinal direction of the wood was found to be approximately 2930 m/s at 4.5 kHz and 5830 m/s at 200 kHz, while for the blocks subjected to 12 weeks of decay, the velocities measured in the longitudinal direction were approximately 2260 m/s to 4120 m/s for 4.5 kHz to 200 kHz, respectively. Also, for the control blocks, the attenuation coefficient magnitudes were found to range from 0.007 to 0.015 Np/mm in the longitudinal direction, 0.028 to 0.052 Np/mm in the radial direction and 0.050 to 0.075 Np/mm in the tangential direction for the frequency range of 4.5 to 200 kHz, respectively, while for the blocks subjected to 12 weeks of decay, the attenuation coefficient magnitudes were found to range from 0.061 to 0.083 Np/mm in the longitudinal direction, 0.199 to 0.265 Np/mm in the radial direction and 0.174 to 0.224 Np/mm in the tangential direction for the same frequency range.

ACKNOWLEDGMENTS

This research was made possible by the ASNT Fellowship Award. The work was also partially supported by the National Science Foundation under Grant No. CMS 02-01305. The wood specimens with controlled decay were prepared at the U.S. Forest Products Laboratory in Madison, Wisconsin.

REFERENCES

ASTM, ASTM D 1413: Standard Test Method for Wood Preservatives by Laboratory Soil-block Cultures, Annual Book of ASTM Standards 4.10, ASTM International, West Conshohocken, Pennsylvania, 2003.

Aebi, L., K Loeffel, J. Bryner, J. Vollmann and J. Dual, "Frequency Selective Wave Propagation in Graded Materials," *IEEE Ultrasonics Symposium Proceedings*, 2007, pp. 1625–1628.

Beall, F.C., J.M. Biernacki and R.L. Lemaster, "The Use of Acousto-ultrasonic to Detect Biodeterioration in Utility Poles," *Journal of Acoustic Emission*, Vol. 12, No. 1/2, 1994, pp. 55–64.

Bodig J. and B.A. Jayne, *Mechanics of Wood and Wood Composites*, Krieger Publishing Company, Malabar, Florida, 2003.

Bucur, V. and R.R. Archer, "Elastic Constants for Wood by an Ultrasonic Method," *Wood Science Technology*, Vol. 18, No. 4, 1984, pp. 255–265.

Bucur, V., *Acoustics of Wood*, 2nd ed., Springer, New York, New York, 2006.

Chiu, T.-C. and F. Erdogen, "One-dimensional Wave Propagation in a Functionally Graded Elastic Medium," *Journal of Sound and Vibration*, Vol. 222, No. 3, 1999, pp. 453–487.

Cowling, E.B., "Comparative Biochemistry of the Decay of Sweetgum Sapwood by White-rot and Brown-rot Fungi," USDA Technical Bulletin 1258, U.S. Department of Agriculture, Washington, D.C., 1961.

Curling, S.F., C.A. Clausen and J.E. Winandy, "Relationships Between Mechanical Properties, Weight Loss, and Chemical Composition of Wood during Incipient Brown-rot Decay," *Forest Products Journal*, Vol. 52, 2002, pp. 34–39.

Eaton, R.A. and M.C.D. Hale, *Wood: Decay, Pests, and Protection*, Chapman and Hall, London, United Kingdom, 1993.

Goodell, B. and G. Xu, "Mechanisms of Wood Degradation by Brown-rot Fungi: Chelator-medicated Cellulose Degradation and Binding of Iron by Cellulose," *Journal of Biotechnology*, Vol. 87, No. 1, 2001, pp. 43–57.

Goodell, B., "Brown-rot Fungal Degradation of Wood: Our Evolving View," *Wood Deterioration and Preservation, ACS Symposium Series*, American Chemical Society, Washington, D.C., 2003.

Green III, F. and T.L. Highley, "Mechanisms of Brown-rot Decay: Paradigm or Paradox," *International Biodeterioration and Biodegradation*, Vol. 39, 1996, pp. 113–124.

Highley, T.L., "Requirements for Cellulose Degradation by Brown-rot Fungus," Material and Organisms, Vol. 11, 1977, pp. 33–46.

Highley, T.L., "Biodeterioration of Wood," *Wood Handbook: Wood as an Engineering Material*, Forest Products Laboratory, Madison, Wisconsin, 1999.

MATLAB, "Least Squares Polynomial Fit," *MATLAB, Help Files*, Math-Works, Cambridge, Massachusetts, 2010.

McSkimin, H.J., "Ultrasonic Measurement Techniques Applicable to Small Solid Specimens," *Journal of the Acoustical Society of America*, Vol. 22, No. 4, 1950, pp. 413–418.

McGovern, M., *Assessment of Brown-rot Decay using x-ray Computer Tomography and Ultrasonic Measurements*, M.S. thesis, University of Illinois at Urbana-Champaign, Urbana, Illinois, 2011.

Papadakis, E.P., "Ultrasonic Attenuation in Thin Specimens Driven through Buffer Rods," *Journal of the Acoustical Society of America*, Vol. 44, No. 3, 1968, pp. 724–734.

Pavlakovic, B. and M. Lowe, *Disperse User's Manual*, Version 2.0.11, Imperial College, London, United Kingdom, 2001.

Proud, J. and P. Tamarkin, "Reflection of Sound from a Surface of Saw-tooth Profile," *Journal of Applied Physics*, Vol. 28, No. 11, 1957, pp. 1298–1301.

Kim, J.Y., M. Treiber and L.J. Jacobs, "A Switching Technique for Measuring High Ultrasonic Attenuation," Review of Quantitative Nondestructive Evaluation, Vol. 28, 2009, pp. 1611–1618.

Kinder, L., A. Frey, h Coppens and J. Sanders, *Fundamentals of Acoustics*, 3rd ed., John Wiley and Sons, Inc., New York, New York, 1980.

Koenigs, W.J., "Fungal Protection of Hydrogen Peroxide in Wood," *Archives of Microbiology*, Vol. 99, 1974, pp. 129–145.

Rose, J.L., Ultrasonic Waves in Solid Media, Cambridge University Press, New York, New York, 1999.

Sachse, W. and Y. Pao, "On the Determination of Phase and Group Velocities of Dispersive Waves in Solids," *Journal of Applied Physics*, Vol. 49, No. 8, 1978, pp. 4320–4327.

Senalik, A, F. Beall and H. Reis, "Detection and Assessment of Wood Decay in Glulam Beams using a Modified Impulse-echo Approach," Insight, Vol. 52, No. 10, 2010, pp. 553–560.

Titta, M., F.C. Beall and J.M. Biernacki, "Acousto-ultrasonic Assessment of Internal Decay in Glulam Beams," *Wood and Fiber Science*, Vol. 30, No. 3, 1998, pp. 259–272.

Vollmann, J., D.M. Profunser, J. Bryner and J. Dual, "Elastodynamic Wave Propagation in Graded Materials: Simulations, Experiments, Phenomena, and Applications," *Ultrasonics*, Vol. 44, 2006, pp. e1215–e1221.